HHS Public Access

Author manuscript

Eur J Immunol. Author manuscript; available in PMC 2018 November 01.

Published in final edited form as:

Eur J Immunol. 2017 November ; 47(11): 1890–1899. doi:10.1002/eji.201747113.

Immunization with a T cell-dependent protein antigen adjuvanted with DOTAP-CpG-B but not DOTAP-CpG-A induces robust germinal center responses and high affinity antibodies

Munir Akkaya[1,*], **Billur Akkaya**[2], **Patrick W. Sheehan**[1], **Pietro Miozzo**[1,**], **Mirna Pena**[1], **Chen-Feng Qi**[1], **Javier Manzella-Lapeira**[1], **Silvia Bolland**[1], and **Susan K. Pierce**[1,*]

[1]Laboratory of Immunogenetics, National Institute of Allergy and Infectious Diseases, National Institutes of Health, Rockville, MD 20852, USA

[2]Laboratory of Immunology, National Institute of Allergy and Infectious Diseases, National Institutes of Health, Bethesda, MD 20892, USA

Abstract

The development of vaccines for infectious diseases for which we currently have none, including HIV, will likely require the use of adjuvants that strongly promote germinal center responses and somatic hypermutation to produce broadly neutralizing antibodies. Here we compared the outcome of immunization with the T-cell dependent antigen, NP-conjugated to chicken gamma globulin (NP-CGG) adjuvanted with the toll-like receptor 9 (TLR9) ligands, CpG-A or CpG-B, alone or conjugated with the cationic lipid carrier, DOTAP. We provide evidence that only NP-CGG adjuvanted with DOTAP-CpG-B was an effective vaccine in mice resulting in robust germinal center responses, isotype switching and high affinity NP-specific antibodies. The effectiveness of DOTAP-CpG-B as an adjuvant was dependent on the expression of the TLR9 signaling adaptor MyD88 in immunized mice. These results indicate DOTAP-CpG-B but not DOTAP-CpG-A is an effective adjuvant for T cell-dependent protein antigen-based vaccines.

Keywords

CpG; TLR 9; DOTAP; Germinal center; Affinity maturation

Introduction

Many vaccines in development for infectious diseases including HIV and malaria are based on purified or recombinant subunit proteins that induce antibodies (Abs) that block infection of target cells [[1–3]]. To induce protective and broadly neutralizing immunity vaccines may

[*]Address correspondence to Susan K. Pierce (spierce@nih.gov) and Munir Akkaya (munir.akkaya@nih.gov), NIH/NIAID/LIG, 12441 Parklawn Drive, Rockville, MD 20852, USA. Phone: (301) 480-3875; Fax: (301) 402-0259.

[**]Current Address: University of Massachusetts Medical School, Worcester, MA 01655

Author Contributions

MA, SKP conceived the project. SKP secured the funding, MA, BA, PM, PWS, performed the experiments. MA, BA, CQ, SB, JM, SKP analyzed the data. MP provided technical help, MA wrote the manuscript, SKP edited the manuscript.

Conflict of Interest

The authors declare no conflicts of interests.

need to induce robust germinal center (GC) responses and high levels of somatic hypermutation, particularly in the case of HIV [4]. However, purified proteins are poorly immunogenic and require delivery with highly effective adjuvants capable of stimulating GC responses. Most, if not all, adjuvants enhance antibody responses by engaging pattern recognition receptors (PRR) of the innate immune system either expressed by cells of the innate immune system or by B cells themselves [5]. Among PRRs, ligands for the Toll-like receptors (TLRs) have received particular attention as adjuvants, including TLR9 ligands. TLR9 is expressed by a variety of cells of the innate and adaptive immune system including dendritic cells (DCs), plasmacytoid DCs (pDCs) and B cells [6]. Upon binding its ligand, microbial DNA containing unmethylated CpG sequences, TLR9 triggers a signaling cascade that promotes a variety of cell functions including survival, proliferation, differentiation and cytokine production [7, 8]. To enhance their potency, synthetic analogs of TLR9 ligands have been generated by embedding CpG motifs into various structurally distinct oligonucleotide (ODN) sequences [9]. These 15-25 nucleotides long synthetic analogs contain one or more CpG sequences and are resistant to nucleases due to partial or full replacement of the phosphodiester bonds with phosphorothioate bonds [10]. Among these analogs, CpG-A and CpG-B are the best studied and commonly used ODNs. CpG-A ODNs are partially phosphorothioate reinforced, and generally contain one CpG motif, and a 3' poly G tail. They form 3D hairpin structures and have tendency to aggregate in salt containing solutions. On the other hand CpG-B ODNs contain more than one CpG motif, are fully phosphorothioate reinforced, do not form complex 3D structure, and are highly soluble [11, 12].

A functional dichotomy has emerged between CpG-A and CpG-B ODNs with CpG-A ODNs being potent stimulants of type-1 interferon (type-1 IFN) production in innate immune cells in particular plasmocytoid DCs (pDCs) and CpG B ODNs enhancing cellular proliferation and proinflammatory cytokine secretion in B cells and in cell types other than pDC [13, 14]. Due to these differences in the functional outcomes, CpG-A has been studied as a modulator of interferon production whereas CpG-B has been considered as a candidate adjuvant to boost innate and adaptive immune responses [12, 13, 15]. However, we recently provided evidence that this dichotomy is not absolute showing that both CpG-B and CpG-A activated B cells to proliferate, secrete Abs and IL-6 *in vitro* and that neither CpG-B nor CpG-A alone induced type 1 IFN production. On the other hand when CpG-A was conjugated with a cationic lipid namely N-[1-(2,3-Dioleoyloxy)propyl]-N,N,N-trimethylammonium methyl-sulfate (DOTAP), we observed induction of type 1 IFN production in B cells both *in vivo* and *in vitro* [16].

There are several additional examples of the modulation of functions of CpG ODNs by conjugation to carriers that affect the trafficking, potency, durability and cellular target of the ODN. For example, conjugation of CpG-B with antigen or antigen-containing nanoparticles boosts its adjuvant effect, resulting in higher Ab responses and memory recall response *in vivo* [17–19]. On the other hand, as commented on above, conjugation of CpG-A with DOTAP confers the ability to initiate type I interferon production in cells such as conventional DCs, macrophages and B cells that do not respond to CpG-A alone [13, 16, 20]. Although the precise mechanism is yet to be elucidated, DOTAP might function to broaden the activity of CpG-A by concentrating it in cells, altering its trafficking to TLR9-

containing compartments in cells or extending its half life in cells. Although this effect of DOTAP conjugation on CpG-A mediated induction of Type-1 IFN production is relatively well established the effect of CpG-DOTAP conjugate on other immune functions and the effect of DOTAP conjugation on the function of CpG-B ODNs are far less well characterized. Indeed, the results of Hou *et. al.*[21], suggest that CpG-B DOTAP conjugates may potentiate Ab responses *in vivo.*

Here, we present the results of an extensive comparative analysis of the efficacy of CpG-A and CpG-B either alone or conjugated to DOTAP as an adjuvant for Ab responses to immunization with the T cell-dependent protein antigen NP-CGG. Our data reveal that neither CpG-A nor CpG-B in their unconjugated forms are potent adjuvants. On the other hand, immunization of mice with DOTAP-CpG-B conjugates but not DOTAP-CpG-A results in strong GC formation, generation of isotype switched Ab producing B cells and production of high affinity Abs in a MyD88-signaling dependent fashion. These findings further our understanding of the role of TLR9 in Ab responses and reveal previously unappreciated functions of cationic lipids in potentiating the adjuvant effects of TLR9 ligands.

Results

CpG-B DOTAP conjugates enhance GC formation in response to T-cell dependent antigens in vivo

To explore the ability of CpG-A, CpG-B and their DOTAP conjugates to function as adjuvants for the response to the T-cell-dependent antigen, NP-CGG, *in vivo*, mice were immunized with NP-CGG alone or with CpG-A, CpG-B or their DOTAP conjugates. DOTAP conjugated directly to NP-CGG resulted in precipitation of the antigen and thus this control was not included. Mice were euthanized 14 days post immunization, spleens were removed, and total GC B cells and NP-specific GC B cells were identified and quantified by a commonly used gating strategy [22–27] as shown (Supplementary Figure 1). T follicular helper (Tfh) cells were also determined by flow cytometry using the gating strategy shown (Supplementary Figure 1). Only mice immunized with CpG-B-DOTAP NP-CGG showed significant increases in the numbers of GC B cells (Figure 1A,C), NP-specific GC B cells (Figure 1D) and Tfh cells (Figure 1B,E) as compared to unimmunized mice or mice immunized with NP-CGG alone or NP-CGG adjuvanted with either CpG-A or CpG-B alone or CpG-A-DOTAP (Figure 1).

Immunization with CpG-B-DOTAP adjuvanted antigens lead to increased GC size, number and proliferative activity

Spleen sections from mice immunized as in Figure 1 were analyzed by immunohistochemistry using: H&E staining to define the splenic architecture; Abs specific for CD3 and B220 to localize follicles; Abs specific for CD4 to identify helper T cells within the follicles (Tfh cells); PNA and Abs specific for IgM to define GCs; and Ki67 to detect proliferating cells in follicles. Representative images of spleen sections are shown (Figure 2A) as well as quantification of the numbers of GCs, the size of GCs and the number of Ki67-positive cells (Figure 2B–D). CpG-B-DOTAP was the most potent adjuvant for NP-CGG, generating the largest number of GCs, GCs of the largest size as well as the greatest

number of Ki-67-positive follicular cells. Immunization with NP-CGG adjuvanted with CpG-A-DOTAP or CpG-B alone also resulted in an increase in the number and size of GCs, as compared to immunization with NP-CGG alone albeit to a lesser extent to that of immunization with NP-CGG CpG-B-DOTAP.

Immunization with DOTAP-CpG-B NP-CGG enhanced the generation of isotype switched antibody producing B cells

We also assessed the expansion of PCs and PBs by flow cytometry defined as $CD138^{Hi}$ and $B220^{Lo}$ to $B220^{-}$ cells (Supplemental Figure 1) in splenocytes harvested 14 days post immunization. Although immunization with NP-CGG CpG-B DOTAP did not have an impact on the total number of PCs/PBs (Figure 3A,C), when spleen cells were placed on ELISPOT plates coated with either NP(30)-BSA to detect NP-specific Ab secreting cells of all affinities (Figure 3B,D) or with NP(4)-BSA to detect high affinity NP-specific Ab secreting cells (Figure 3B,E), the total number of NP-specific Ab secreting cells (Figure 3 B,D) and high affinity NP-specific Ab secreting cells (Figure 3B,E) increased only in the spleens of mice immunized with NP-CGG CpG-B-DOTAP in comparison to unimmunized mice or mice immunized with NP-CGG.

The total amount of NP-specific Ab was measured in serum collected from mice immunized as described in Figure 1, seven and 14 days post immunization (Figure 4A,B). The total NP-specific IgM response seven days post immunization, as measured by NP(30)-BSA ELISAs, was higher in mice that received NP-CGG adjuvanted with either CpG-A-DOTAP or CpG-B-DOTAP as compared to mice that received NP-CGG alone or NP-CGG adjuvanted with CpG-A or CpG-B (Figure 4A). However, the effect of these adjuvants was not evident 14 days after immunization, a time at which all responses were more or less equivalent (Figure 4B). In contrast, NP-CGG adjuvanted with CpG-B-DOTAP induced higher levels of IgG Ab that were of greater affinity on day 7 post immunization and persisted to day 14 post immunization as compared to all other immunogens.

The adjuvant effect of CpG-B-DOTAP is dependent on TLR9 signaling

Finally, we ruled out the possibility that the enhanced adjuvant activity of DOTAP-CpG-B was not due to TLR9 signaling but to a modification or multimerization of NP-CGG in the presence of DOTAP. The dependence of the effectiveness of CpG-B-DOTAP on TLR9 signaling was tested by immunizing WT and TLR9 signaling-deficient (MyD88 KO) mice either with NP-CGG or NP-CGG adjuvanted with CpG-B-DOTAP. Spleens were removed at day 14 post immunization and the total numbers of GC, NP-specific GC and Tfh, were determined by flow cytometry (Fig. 5A–E). The number of NP-specific Ab secreting cells was determined by ELISPOT (Fig. 5F, G). For all parameters, immunization with NP-CGG DOTAP-CpG-B generated a significantly better response in WT mice as compared to MyD88 KO mice, confirming the dependence of the observed phenotypes on TLR9 signaling.

Discussion

Immune responses to T-cell-dependent antigens are complex processes that involve multiple cell types and mediators of the immune system [28, 29]. The initiation of T-cell-dependent

Ab responses occurs in lymphoid organs at the T-B border and continues in the specialized micro-environment of the GCs where B cells rapidly proliferate undergo class switching and somatic hypermutation and are selected based on their affinity for the antigen [30]. Recent advances in high resolution imaging methods *in vivo* have provided a wealth of new information concerning the cellular and molecular mechanisms that underlie GC reactions [31]. Since the ultimate goal of this process is the production of long-lasting, potent, specific Abs, the generation of adjuvants that can facilitate these outcomes is a high priority in clinical studies.

TLR9 is expressed in the majority of the cells involved in GC reactions, and is a candidate target for adjuvant development [32]. Therefore, synthetic analogs of its ligands are continuously tested in various immunization regimes [33]. Although studies *in vitro* have provided evidence that CpG-B is a potent stimulant of DC functions as well as of B cell proliferation, antibody production and differentiation into plasma cell lineage, whether CpG-B has these effects *in vivo* is not as clear. This may be due to a large number of factors including the failure to reach high enough concentrations at the target organ and or the rapid clearance of this relatively simple structure from the body [34]. Therefore modifications that would prolong the response or potentiate it by concentrating ODNs are desired.

Here we showed that DOTAP conjugation of CpG-B is a practical strategy to boost multiple elements of the T cell-dependent immune response. Mice immunized with antigens adjuvanted with DOTAP conjugated CpG-B showed enhancement in various aspects of immune response including the number of total and antigen-specific GC B cells, GC size, number of Tfh cells, number of specific Ab-producing cells and serum levels for both total and high affinity Abs specific for the antigen. On the other hand CpG-A conjugation of DOTAP resulted only in a slight increase in GC size and early Ab response in the form of IgM, yet failed to propagate other aspects of the immune response.

By comparing DOTAP conjugates of CpG-A and CpG-B and demonstrating the remarkable difference in their effects on T cell-dependent immune response, we highlight the importance of CpG ODN type in the outcome of TLR9 signaling. Although this phenomenon has been studied in detail in the context of interferon secretion, we provide the first evidence for its relevance in *in vivo* immunization settings as well.

The failure to observe any significant effect by using unconjugated CpG as adjuvants, highlights the need for additional mediators or conjugation strategies to reveal the effect. Although it can be argued that using a higher concentration of CpG and or administration of it in multiple doses might facilitate an unconjugated CpG mediated adjuvant effect, these may also increase potential off-target effects and generate unexpected outcomes.

DOTAP conjugated CpG ODNs have been reported to induce both TLR dependent and independent outcomes in several previous studies [35, 36]. Although the actual mechanism by which DOTAP mediates TLR independent effect is not clear it might be due to the altered intracellular uptake and trafficking of ODNs by DOTAP making them more accessible to cytoplasmic DNA sensors. However, using MyD88 KO mice, we showed that the

immunoadjuvant effect of CpG-B DOTAP conjugate is dependent in large part on TLR9 signaling.

The mechanisms by which DOTAP enhance the adjuvant properties of CpG-B remain to be elucidated, but potential explanations include DOTAPs prevention of premature degradation of CpG-B. Another likely explanation is the formation of multimeric CpG complexes or bridging the antigen to the adjuvant. Although our experimental design involves conjugating CpG- DOTAP first and then adding the antigen to prevent clumping of the antigen by DOTAP, interactions betwen DOTAP-CpG and the antigen might be taking place and the resulting complex might be gaining increased potency. Pursuing the mechanism of the success of DOTAP-CpG-B as an adjuvant for T-cell dependent antigens may lead to new strategies to improve the adjuvant properties of CpG-B.

Materials and Methods

Animals

WT (C57BL/6) and Myd88 KO mice (*B6.129P2(SJL)-Myd88tm1.1Defr/J*) were purchased from Jackson Laboratory (Bar Harbor, ME, USA). All mice were maintained at the National Institutes of Health animal facilities in compliance with Animal Care and Use Committee standards.

Immunizations

CpG-A (ODN1585) and CpG-B (ODN1826) ODNs were purchased from Invivogen (San Diego, CA, USA). For conditions involving cationic lipid-ODN complexes, N-[1-(2,3-Dioleoyloxy)propyl]-N,N,N-trimethylammonium methyl-sulfate (DOTAP), a cationic lipid based liposomal transfection reagent (Roche, Basel, Switzerland) was used. For this purpose, ODNs and DOTAP were added into HBS (Sigma-Aldrich, St. Louis, MO, USA) in separate tubes at the desired amounts. These solutions were mixed without agitation and the resulting DOTAP-ODN mixture was incubated at RT for 15-20 minutes before being mixed with the antigen just prior to injecting the mice.

Intraperitoneal injections of mice were performed using 300 μl/mouse sterile HBS solution containing 4-Hydroxy-3-nitrophenylacetyl hapten conjugated Chicken Gamma Globulin (NP-CGG) and ODNs (DOTAP conjugated or unconjugated). NP-CGG used in these experiments was at a ratio of approximately 18 NP to 1 CGG and purchased from Biosearch Technologies (Novato, CA, USA). Intraperitoneal injection of NP-CGG-Alum was carried out using 100 μg/mouse NP-CGG (dissolved in 200 μl/mouse PBS) conjugated with 100 μl/mouse Imject Alum (ThermoFisher).

ELISAs

Measurement of anti-NP antibodies was carried out by applying different dilutions of the mouse serum onto plates that were previously coated with 10 μg/ml NP-BSA (LGC Biosearch) complexes. NP to BSA ratio of 4 and 30 were used to detect high and mixed affinity antibodies respectively. HRP conjugated anti mouse IgG or IgM were used as secondary antibodies. Plates were developed using TMB buffer (eBioscience), reaction was

quenched using 0.18M H_2SO_4 and plates were read at 450 nm wavelength. Serum pooled from five different NP-CGG-Alum injected mice (14 days post injection) was serially diluted in order to generate an arbitrary unit scale. This unit scale was used to standardize absorbance values obtained from different plates.

ELISPOT

To detect the NP specific PCs in the spleens of NP-CGG immunized mice, 96 well sterile filter plates (MSIPS4W10- Millipore, Billerica, MA, USA) were coated with 10 μg/ml NP-BSA in sterile PBS over night at 4 °C. To discriminate the affinity of interactions, NP:BSA ratios of 4 (high affinity) and 30 (mixed affinity) were used. Plates were washed three times with PBS and then blocked with sterile PBS supplemented with 1% BSA for 2 hours at RT Followed by another three washes with sterile PBS. Cells harvested from the spleens of mice on day 14 post immunization were resuspended at three different dilutions in serum free X-VIVO™ 20 media (Lonza) supplemented with β-ME and plated into the ELISPOT plate. Plates were incubated at 37 °C, in a 5% CO_2 incubator, avoiding any vibrations for 20-24 hours. Cells were then discarded and plates were washed three times with PBS followed by another three washes with PBS-Tween 20 (0.5%). HRP-conjugated anti mouse IgG in PBS-Tween 20 (0.5%)-BSA (1%) solution was added to the plates. Following overnight incubation at 4°C, Plates were washed three times with PBS-Tween 20 (0.5%) followed by another three washes with PBS alone. Plates were developed using an AEC substrate kit (BD Biosciences) according to manufacturer's guidelines. Evaluation and imaging of the developed ELISPOT plates were carried out by Zellnet Consulting, Fort Lee, NJ, USA.

Histopathologic evaluation of spleen

Spleens were harvested 14 days after intraperitoneal immunization of mice. Spleens were immediately fixed in 10% buffered formalin and embedded in paraffin. Tissue sections were prepared and stained either by hematoxylin and eosin (H&E) to define splenic architecture or by immunostaining according to standard protocols, and examined by light microscopy with magnifications of 5×, 10×, and 20×. Immunostaining was performed by carrying out the avidin-biotin peroxidase complex (ABC) method, using the Vectastain Elite ABC kit (Vector Labs, Burlingame, CA, USA) according to the manufacturer's instructions. Abs specific for CD3 (#MCA1477) (AbDSerotec, Oxford, UK) and B220 (#553086) (BD Bioscience) were used to distinguish T and B cells respectively in follicles. PNA (PNA-biotin conjugated, #B-1075) (Vector Labs), and Abs specific for IgM (#A-20144) (ThermoFisher) were used to define GCs, Abs specific for CD4 (#17-0031-82) (eBioscience) identified Tfh cells and Ki-67 (#M0879) (DAKO, Carpinteria, CA, USA) was used to identify proliferating cells.

Quantification of the GC size and the number of Ki-67 stained follicular cells per spleen section was done by analysis of images of individual spleen sections from spleens from two different mice per condition at 20× magnification. For the image processing, we developed a program with MATLAB (MathWorks, Natick, MA USA). In order to facilitate the identification of positive stained cells, we first separated the images into their red-blue-green, hue, saturation, and value components to make binary masks. Masks were further

refined by dilation/erosion filtration. We then applied an algorithm to segment the regions detailed in the masks, with a customized watershed procedure .

Flow cytometry

Samples were stained for flow cytometry in FACS buffer (HBSS supplemented with, 1% HEPES, 2% FCS and 10mM Sodium Azide (Sigma-Aldrich) on ice using antibodies/stains listed in Supplementary Table 1.

Flow cytometry experiments were carried out using BD LSR-II Cytometer and data were analyzed in FlowJo software.

Statistical analyses

Statistical analyses were carried out in Graphpad Prism software. Unpaired t-test with Welch's correction was used to determine the significance of the difference observed. ($P>0.05$ = ns; $0.01 <P \leq 0.05$ = *; $0.001 <P \leq 0.01$ = **; $0.0001 <P \leq 0.001$ = ***; $P \leq 0.0001$= ****).

Supplementary Material

Refer to Web version on PubMed Central for supplementary material.

Acknowledgments

This study was supported by the Intramural Research Program of the National Institutes of Health, National Institute of Allergy and Infectious Diseases. Authors thank Dr. Hongsheng Wang (NIH) for advice on ELISA and ELISPOT experiments.

References

1. Cleland JL, Powell MF, Lim A, Barron L, Berman PW, Eastman DJ, Nunberg JH, Wrin T, Vennari JC. Development of a single-shot subunit vaccine for HIV-1. AIDS Res Hum Retroviruses. 1994; 10(Suppl 2):S21–26. [PubMed: 7865303]
2. Moorthy VS, Kieny MP. Reducing empiricism in malaria vaccine design. Lancet Infect Dis. 2010; 10:204–211. [PubMed: 20185099]
3. Garcon N, Heppner DG, Cohen J. Development of RTS, S/AS02: a purified subunit-based malaria vaccine candidate formulated with a novel adjuvant. Expert Rev Vaccines. 2003; 2:231–238. [PubMed: 12899574]
4. Streeck H, D'Souza MP, Littman DR, Crotty S. Harnessing CD4(+) T cell responses in HIV vaccine development. Nat Med. 2013; 19:143–149. [PubMed: 23389614]
5. Coffman RL, Sher A, Seder RA. Vaccine adjuvants: putting innate immunity to work. Immunity. 2010; 33:492–503. [PubMed: 21029960]
6. Kumagai Y, Takeuchi O, Akira S. TLR9 as a key receptor for the recognition of DNA. Adv Drug Deliv Rev. 2008; 60:795–804. [PubMed: 18262306]
7. Rutz M, Metzger J, Gellert T, Luppa P, Lipford GB, Wagner H, Bauer S. Toll-like receptor 9 binds single-stranded CpG-DNA in a sequence- and pH-dependent manner. Eur J Immunol. 2004; 34:2541–2550. [PubMed: 15307186]
8. Hemmi H, Takeuchi O, Kawai T, Kaisho T, Sato S, Sanjo H, Matsumoto M, Hoshino K, Wagner H, Takeda K, Akira S. A Toll-like receptor recognizes bacterial DNA. Nature. 2000; 408:740–745. [PubMed: 11130078]
9. Klinman D, Shirota H, Tross D, Sato T, Klaschik S. Synthetic oligonucleotides as modulators of inflammation. J Leukoc Biol. 2008; 84:958–964. [PubMed: 18430787]

10. Sester DP, Naik S, Beasley SJ, Hume DA, Stacey KJ. Phosphorothioate backbone modification modulates macrophage activation by CpG DNA. J Immunol. 2000; 165:4165–4173. [PubMed: 11035048]
11. Avalos AM, Latz E, Mousseau B, Christensen SR, Shlomchik MJ, Lund F, Marshak-Rothstein A. Differential cytokine production and bystander activation of autoreactive B cells in response to CpG-A and CpG-B oligonucleotides. J Immunol. 2009; 183:6262–6268. [PubMed: 19864612]
12. Bode C, Zhao G, Steinhagen F, Kinjo T, Klinman DM. CpG DNA as a vaccine adjuvant. Expert Rev Vaccines. 2011; 10:499–511. [PubMed: 21506647]
13. Honda K, Ohba Y, Yanai H, Negishi H, Mizutani T, Takaoka A, Taya C, Taniguchi T. Spatiotemporal regulation of MyD88-IRF-7 signalling for robust type-I interferon induction. Nature. 2005; 434:1035–1040. [PubMed: 15815647]
14. Gursel M, Verthelyi D, Gursel I, Ishii KJ, Klinman DM. Differential and competitive activation of human immune cells by distinct classes of CpG oligodeoxynucleotide. J Leukoc Biol. 2002; 71:813–820. [PubMed: 11994506]
15. Verthelyi D, Kenney RT, Seder RA, Gam AA, Friedag B, Klinman DM. CpG oligodeoxynucleotides as vaccine adjuvants in primates. J Immunol. 2002; 168:1659–1663. [PubMed: 11823494]
16. Akkaya M, Akkaya B, Miozzo P, Rawat M, Pena M, Sheehan PW, Kim AS, Kamenyeva O, Kabat J, Bolland S, Chaturvedi A, Pierce SK. B Cells Produce Type 1 IFNs in Response to the TLR9 Agonist CpG-A Conjugated to Cationic Lipids. J Immunol. 2017
17. de Titta A, Ballester M, Julier Z, Nembrini C, Jeanbart L, van der Vlies AJ, Swartz MA, Hubbell JA. Nanoparticle conjugation of CpG enhances adjuvancy for cellular immunity and memory recall at low dose. Proc Natl Acad Sci U S A. 2013; 110:19902–19907. [PubMed: 24248387]
18. Bourquin C, Anz D, Zwiorek K, Lanz AL, Fuchs S, Weigel S, Wurzenberger C, von der Borch P, Golic M, Moder S, Winter G, Coester C, Endres S. Targeting CpG oligonucleotides to the lymph node by nanoparticles elicits efficient antitumoral immunity. J Immunol. 2008; 181:2990–2998. [PubMed: 18713969]
19. Rookhuizen DC, DeFranco AL. Toll-like receptor 9 signaling acts on multiple elements of the germinal center to enhance antibody responses. Proc Natl Acad Sci U S A. 2014; 111:E3224–3233. [PubMed: 25053813]
20. Sasai M, Linehan MM, Iwasaki A. Bifurcation of Toll-like receptor 9 signaling by adaptor protein 3. Science. 2010; 329:1530–1534. [PubMed: 20847273]
21. Hou B, Saudan P, Ott G, Wheeler ML, Ji M, Kuzmich L, Lee LM, Coffman RL, Bachmann MF, DeFranco AL. Selective utilization of Toll-like receptor and MyD88 signaling in B cells for enhancement of the antiviral germinal center response. Immunity. 2011; 34:375–384. [PubMed: 21353603]
22. Bollig N, Brustle A, Kellner K, Ackermann W, Abass E, Raifer H, Camara B, Brendel C, Giel G, Bothur E, Huber M, Paul C, Elli A, Kroczek RA, Nurieva R, Dong C, Jacob R, Mak TW, Lohoff M. Transcription factor IRF4 determines germinal center formation through follicular T-helper cell differentiation. Proc Natl Acad Sci U S A. 2012; 109:8664–8669. [PubMed: 22552227]
23. Burbage M, Keppler SJ, Gasparrini F, Martinez-Martin N, Gaya M, Feest C, Domart MC, Brakebusch C, Collinson L, Bruckbauer A, Batista FD. Cdc42 is a key regulator of B cell differentiation and is required for antiviral humoral immunity. J Exp Med. 2015; 212:53–72. [PubMed: 25547673]
24. Cato MH, Chintalapati SK, Yau IW, Omori SA, Rickert RC. Cyclin D3 is selectively required for proliferative expansion of germinal center B cells. Mol Cell Biol. 2011; 31:127–137. [PubMed: 20956554]
25. Collins CM, Speck SH. Expansion of murine gammaherpesvirus latently infected B cells requires T follicular help. PLoS Pathog. 2014; 10:e1004106. [PubMed: 24789087]
26. Moshkani S, Kuzin II, Adewale F, Jansson J, Sanz I, Schwarz EM, Bottaro A. CD23+ CD21(high) CD1d(high) B cells in inflamed lymph nodes are a locally differentiated population with increased antigen capture and activation potential. J Immunol. 2012; 188:5944–5953. [PubMed: 22593620]
27. Shrestha S, Yang K, Guy C, Vogel P, Neale G, Chi H. Treg cells require the phosphatase PTEN to restrain TH1 and TFH cell responses. Nat Immunol. 2015; 16:178–187. [PubMed: 25559258]

28. Jeurissen A, Ceuppens JL, Bossuyt X. T lymphocyte dependence of the antibody response to ‘T lymphocyte independent type 2‘ antigens. Immunology. 2004; 111:1–7. [PubMed: 14678191]
29. Grewal IS, Flavell RA. CD40 and CD154 in cell-mediated immunity. Annu Rev Immunol. 1998; 16:111–135. [PubMed: 9597126]
30. De Silva NS, Klein U. Dynamics of B cells in germinal centres. Nat Rev Immunol. 2015; 15:137–148. [PubMed: 25656706]
31. Allen CD, Okada T, Cyster JG. Germinal-center organization and cellular dynamics. Immunity. 2007; 27:190–202. [PubMed: 17723214]
32. Dowling JK, Mansell A. Toll-like receptors: the swiss army knife of immunity and vaccine development. Clin Transl Immunology. 2016; 5:e85. [PubMed: 27350884]
33. Scheiermann J, Klinman DM. Clinical evaluation of CpG oligonucleotides as adjuvants for vaccines targeting infectious diseases and cancer. Vaccine. 2014; 32:6377–6389. [PubMed: 24975812]
34. Palma E, Cho MJ. Improved systemic pharmacokinetics, biodistribution, and antitumor activity of CpG oligodeoxynucleotides complexed to endogenous antibodies in vivo. J Control Release. 2007; 120:95–103. [PubMed: 17509715]
35. Yasuda K, Ogawa Y, Yamane I, Nishikawa M, Takakura Y. Macrophage activation by a DNA/cationic liposome complex requires endosomal acidification and TLR9-dependent and -independent pathways. J Leukoc Biol. 2005; 77:71–79. [PubMed: 15496451]
36. Yasuda K, Yu P, Kirschning CJ, Schlatter B, Schmitz F, Heit A, Bauer S, Hochrein H, Wagner H. Endosomal translocation of vertebrate DNA activates dendritic cells via TLR9-dependent and -independent pathways. J Immunol. 2005; 174:6129–6136. [PubMed: 15879108]

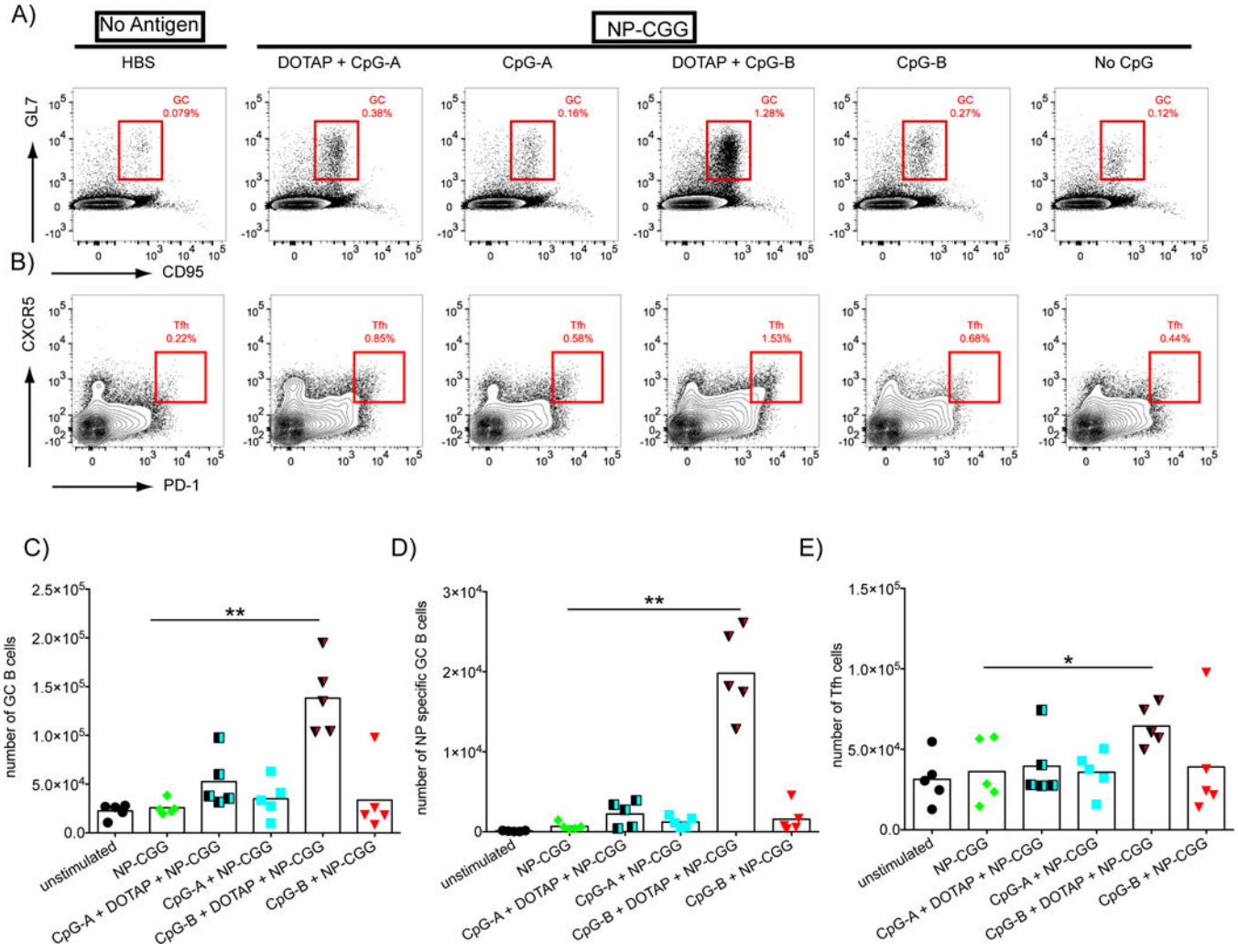

Figure 1.

CpG-B-DOTAP is an effective adjuvant for T cell-dependent antigens. A-B) Mice were immunized intraperitoneally with NP-CGG (100 μg/mouse) either alone or with CpG-A or CpG-B with or without DOTAP (70 μg/mouse CpG +/− 190 μg/mouse DOTAP) in HBS. Control mice received 500 μl HBS only. Spleens were taken 14 days post injection and analyzed by flow cytometry according to the gating strategy described in Supplementary Figure 1. Representative flow cytometry plots indicate the relative frequencies of: A) GC B cells among total B cells or B) Tfh cells among total $CD4^+$ T cells. Total number of: C) GC B cells; D) NP-specific GC B cells and E) Tfh cells are shown. Values that are significantly different from those of mice immunized with NP-CGG alone are shown with asterisks ($0.01 < P \leq 0.05$ = *; $0.001 < P \leq 0.01$ = **) (t-test). Data shown are representatives of three independent experiments each with 5 mice per condition.

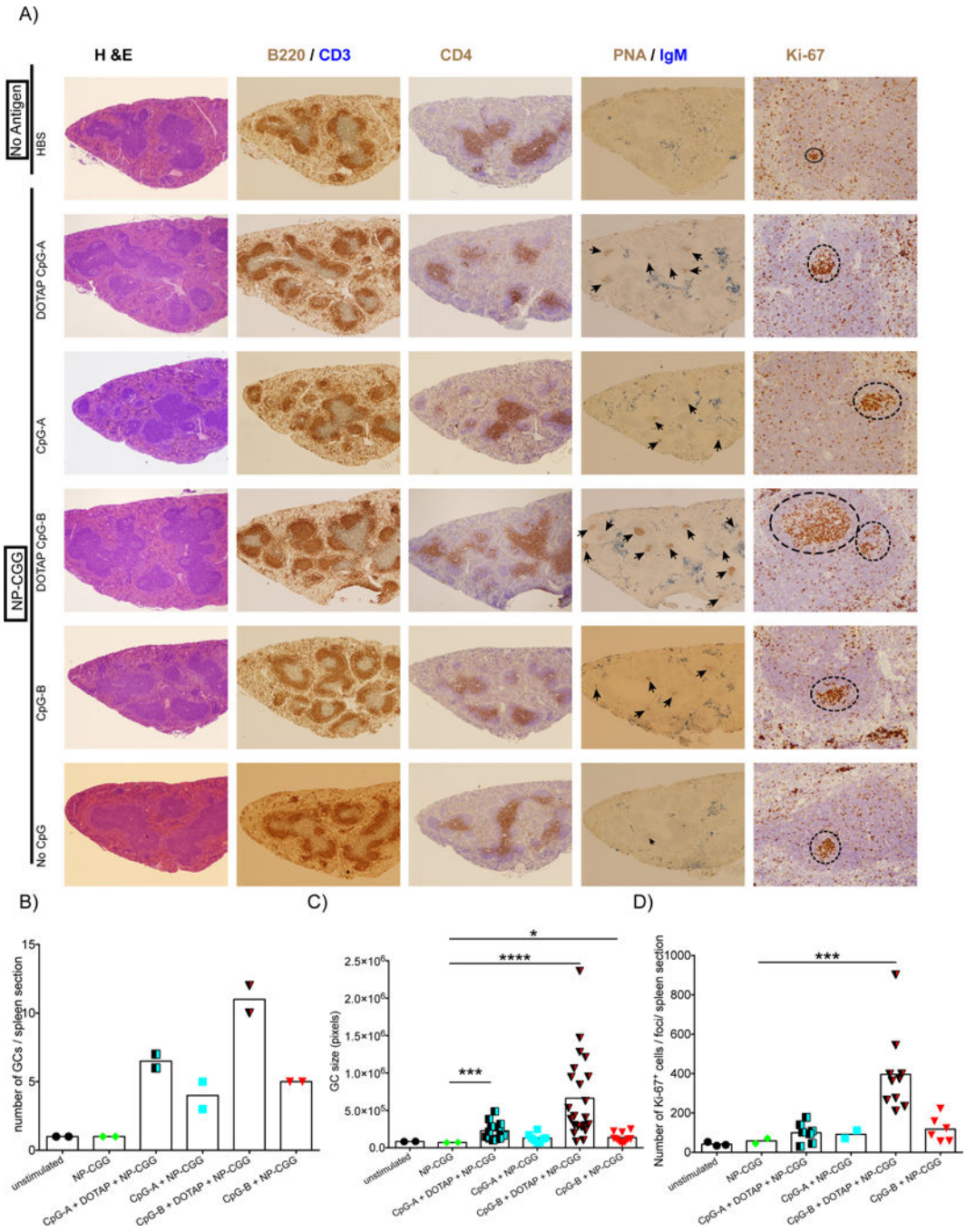

Figure 2.

The effect of immunization with the T-dependent antigen, NP-CGG, adjuvanted with CpG-B- DOTAP on the number and size of GCs and their proliferative activity. A) Fixed and paraffin embedded spleen sections generated from spleens of mice immunized as described in Figure 1 were evaluated using immunohistochemistry. Representative light microscopy images are shown. All images are 5× magnified except for the 20× magnified ones showing the Ki-67 staining of the GCs. In sections stained with both PNA and Abs specific for IgM, black arrowheads indicate the GC foci. In Ki-67 stained samples, dotted circles show areas

of cells with high Ki-67 staining within follicles. The area of GCs and the number of Ki-67-positive cells were quantified as detailed in Materials and Methods. B-D) Graphs show the total number of GC foci (B), GC area (C) and number of Ki-67-positive follicular B cells (D) obtained from individual sections from two different spleens per group. T-test was used to calculate statistical significance (C-D) and values that are significantly different from those of mice immunized with NP-CGG alone are shown with asterisks ($0.01 < P \leq 0.05$ = *; $0.0001 < P \leq 0.001$ = ***; $P \leq 0.0001$=****)

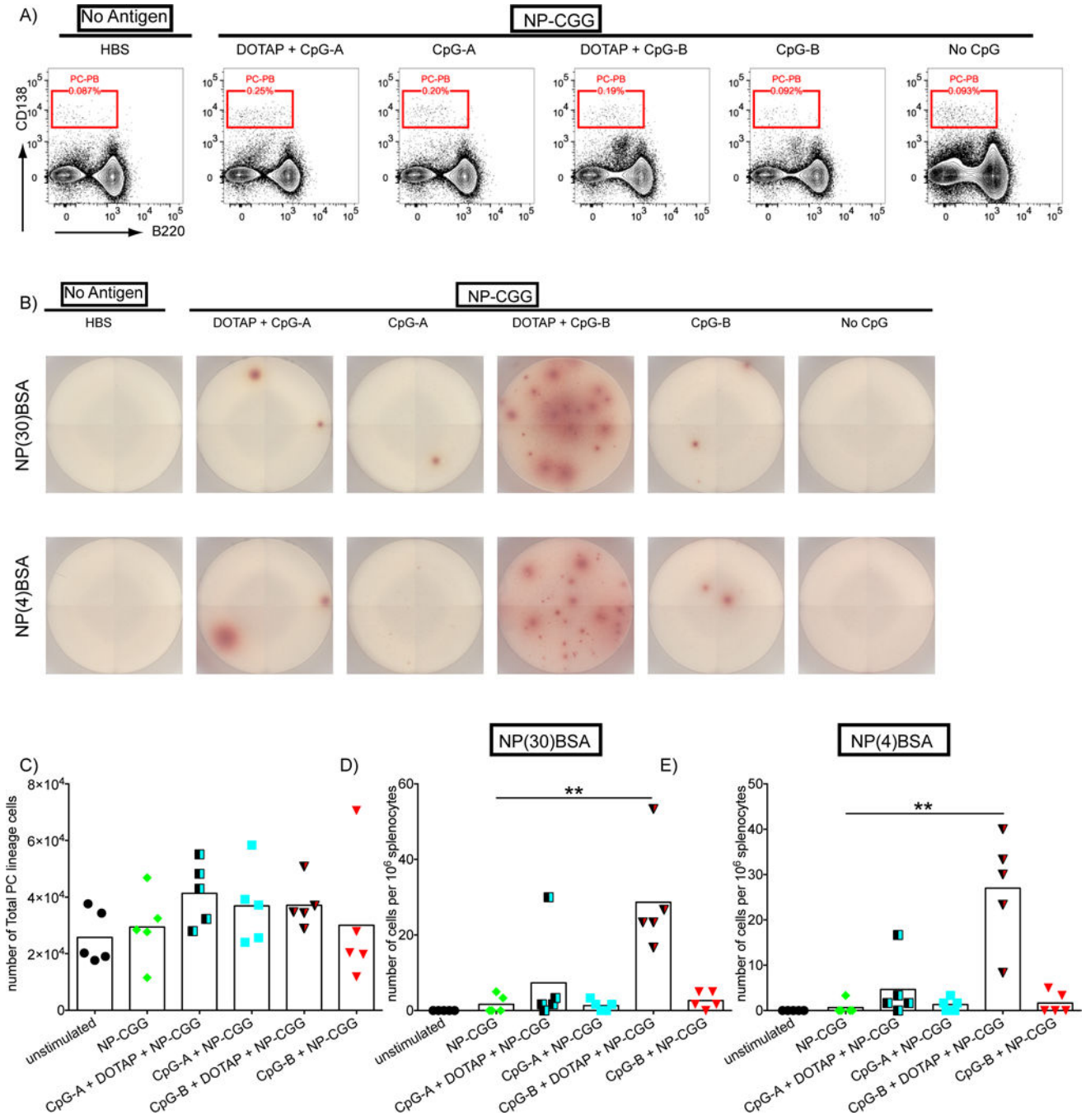

Figure 3.

CpG-B-DOTAP enhances plasma cell generation in response to NP-CGG immunization. WT mice were immunized as described in Figure 1 and spleens were harvested 14 days post injection. A) Flow cytometry plots indicating the frequency of PCs and PBs among live splenocytes are shown. B) Representative images demonstrating the PCs secreting IgG NP-specific Ab, as detected by plating equal numbers of splenocytes on ELISPOT plates coated with either NP(30)BSA (top panel) or NP(4)BSA (bottom panel), are shown. C) Shown are the total numbers of PCs and PBs as detected by flow cytometry, NP-specific PCs as

detected by either (D) NP(30)BSA ELISPOT or (E) NP(4)ELISPOT are shown. Values that are significantly different compared to those of mice immunized with NP-CGG alone are shown with asterisks ($0.01 < P \leq 0.05$ = *; $0.001 < P \leq 0.01$ = **) (t-test). Data represents three independent experiments each containing five mice per group

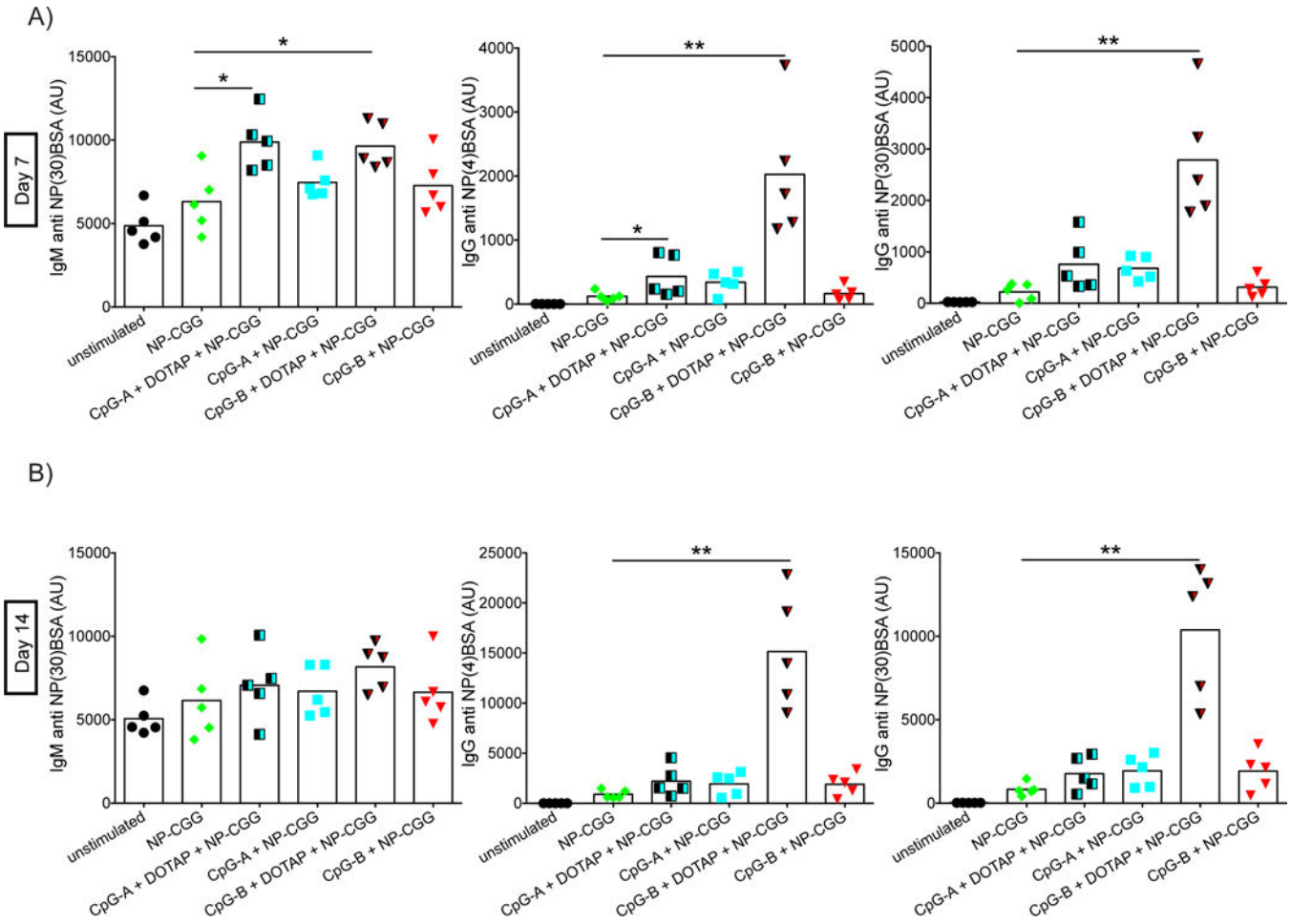

Figure 4.

CpG-B DOTAP increases the serum levels of NP specific antibodies. Changes in the titers of NP specific antibodies in serum of immunized mice were detected by ELISA using blood taken (A) seven and (B) 14 days post immunization. Arbitrary units were calculated using standard dilutions of pooled serum collected from NP-CGG-Alum immunized mice. Values that are significantly different compared to those of mice immunized with NP-CGG alone are shown with asterisks ($0.01 < P \leq 0.05$ = *; $0.001 < P \leq 0.01$ = **) (t-test). Data represents three independent experiments each containing five mice per group.

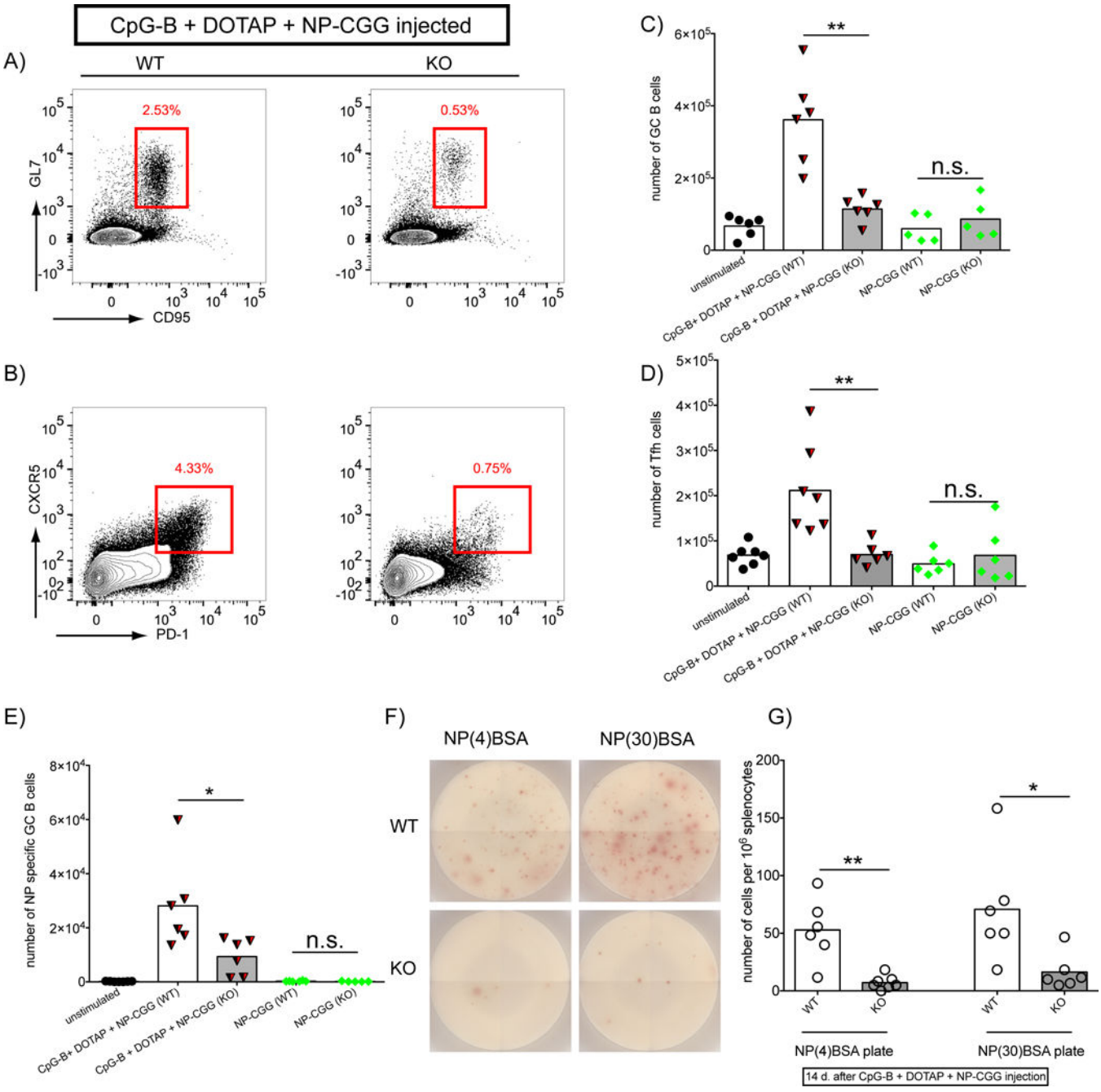

Figure 5.

Adjuvant effects of CpG-B DOTAP are largely dependent on TLR9 signaling. A-E) Age and sex matched WT and MyD88 KO mice were injected with either NP-CGG or NPCGG with DOTAP-CpG-B as explained in Figure 1. Spleens were harvested 14 days post injection and analyzed in flow cytometry. Representative Flow cytometry plots showing GC B cells in B cell gate (A) and Tfh cells in CD4+ T cell gate (B) are shown for DOTAP-CpG-B + NP-CGG injected WT (left) and KO (right) mice. C-D) Total numbers of GC B cells (C), Tfh cells (D), and NP-specific GC B cells (E) are shown. F-G) Equal numbers of splenocytes from the above experiment were plated on NP(4)BSA or NP(30)BSA coated ELISPOT

plates as explained in Figure 3. Plates were developped with anti mouse IgG Representative wells are shown in H and total numbers of spots are ploted in I. ($0.01 < P \leq 0.05$ = *; $0.001 < P \leq 0.01$ = **) (t-test). Data represents two independent experiments each containing at least five mice per group.